doi: 10.37905/jgeosrev.v6i2.24475 ejurnal.ung.ac.id/index.php/jgeosrev

Vol. 6, No. 2, July 2024: 73-84

Jambura Geoscience Review

p-ISSN 2623-0682 | e-ISSN 2656-0380

Department of Earth Science and Technology, Universitas Negeri Gorontalo

Evolution of Sequence Stratigraphy and Paleogeography, Case Study: M2 Member of the Muara Enim Formation

Kevin Nabil Hibatullah[1], Budhi Setiawan[1], Yogie Zulkurnia Rochmana[1], M. Dwiki Satrio Wicaksono[2]

[1] *Geological Engineering, Sriwijaya University, Indralaya, Ogan Ilir, South Sumatra 30862, Indonesia*
[2] *PT. Bukit Asam Tbk., Jl. Parigi No.1., Tajung Enim, Muara Enim, South Sumatra 31716, Indonesia.*

ARTICLE INFO

Article history:
Received: 13 February 2024
Accepted: 22 July 2024
Published: 29 July 2024

Keywords:
Coal, Muara Enim, Paleogeography, Sequence Stratigraphy

Corresponding author:
Yogie Zulkurnia Rochmana
Email:
yogie.zrochmana@ft.unsri.ac.id

ABSTRACT

Sequence stratigraphy related to accommodation space as an area of potential sediment accumulation that is influenced by fluctuations in sea level and subsidence of the basin floor. Paleogeography, on the other hand, is the study of physical geographic features and their evolution throughout geological periods. The aim of this work is to shed light on the relationship between paleogeographic evolution and sequence stratigraphy, as well as coal accumulation in the South Sumatra Basin. The method used are geophysical logs and cores analysis to determine the system tracts, types of system tracts, and stratigraphic sequences, lithofacies and sedimentary facies analysis, paleogeographic analysis using modified single-factor and multi-factor and them mapped using IDW as a geostatistical method. The results indicate that the study area comprises four system tracts, namely TST-1, HST-1, TST-2 and HST-2. In TST-1 and TST-2, the rate of peat formation is balanced with the rate of accommodation space formation, resulting in continuous and very thick coal accumulation. In HST-1 and HST-2, the rate of accommodation space formation exceeds the rate of peat formation, leading to continuous coal accumulation that is quite thick to very thick. Sequence 1 consists of lagoon and tidal/mouth/distal bar paleogeographic unit with sand/shale ratio range 0.217 to 0.247. Sequence 2 consists of lagoon paleogeographic units with sand/shale ratio range 0.046 to 0.05.

How to cite: Hibatullah, K.N. (2024). Evolution of Sequence Stratigraphy and Paleogeography, Case Study: M2 Member of the Muara Enim Formation. *Jambura Geoscience Review, 6*(2), 73-84. https://doi.org/10.37905/jgeosrev.v6i2.24475

1. INTRODUCTION

Sequence stratigraphy describes the accommodation space as the area available for potential sediment accumulation, which is influenced by global sea level fluctuations and basin floor subsidence rather than sediment supply (Lu et al., 2013). Coal accumulation and distribution are not only influenced by sea level changes but also by some factors such as accommodation space, sediment supply, peat accumulation rate, and climate change (Flint, Aitken, and Hampson, 1995; Diessel et al., 2000; Buillit et al., 2002; Opluštil et al., 2013; Bai et al., 2020). Palaeogeography studies geographic, physical features and their evolution throughout geological history (Zeng-Zhao Feng, 1999a, 1999b; Feng et al., 2014).

The research area is geographically located in Tanjung Enim, Muara Enim Regency, South Sumatra, which belongs to the Muara Enim Formation (**Figure 1**). The Muara Enim Formation is a Late Miocene - Early Pliocene age coal-forming formation with lithologies of mudstone, siltstone, sandstone, and coal (Amijaya & Littke, 2005). The formation is divided into Lower MPa (Central

Palembang 'a') and Upper MPb (Central Palembang 'b'), which are further subdivided into M1-M4 members (Shell Mijnbouw, 1976; Amijaya and Littke, 2005). As an important coal-bearing basin, maceral analysis, sedimentary depositional environment, coal accumulation, and tectonic evolution have been investigated in detail (Amijaya and Littke, 2005; Nasution and Nalendra, 2017; Algadri Nafian and Rizal, 2021; Elcofa et al., 2023). However, discussions on the relationship of stratigraphic sequence to palaeogeography and coal accumulation have yet to be conducted in the South Sumatra Basin. Stratigraphic sequence, depositional environment characteristics, and paleogeographic evolution will be discussed, explaining the stratigraphic sequence and coal seam accumulation model in the South Sumatra Basin.

This work aims to shed light on the relationship between palaeogeographic evolution, sequence stratigraphy, and coal accumulation in the South Sumatra Basin. This research is intended to enrich and deepen the theory of coal accumulation and its relationship to stratigraphic sequence and the evolution of past depositional environments in the South Sumatra Basin, as well as predict and calculate the economic coal resources in the South Sumatra Basin.

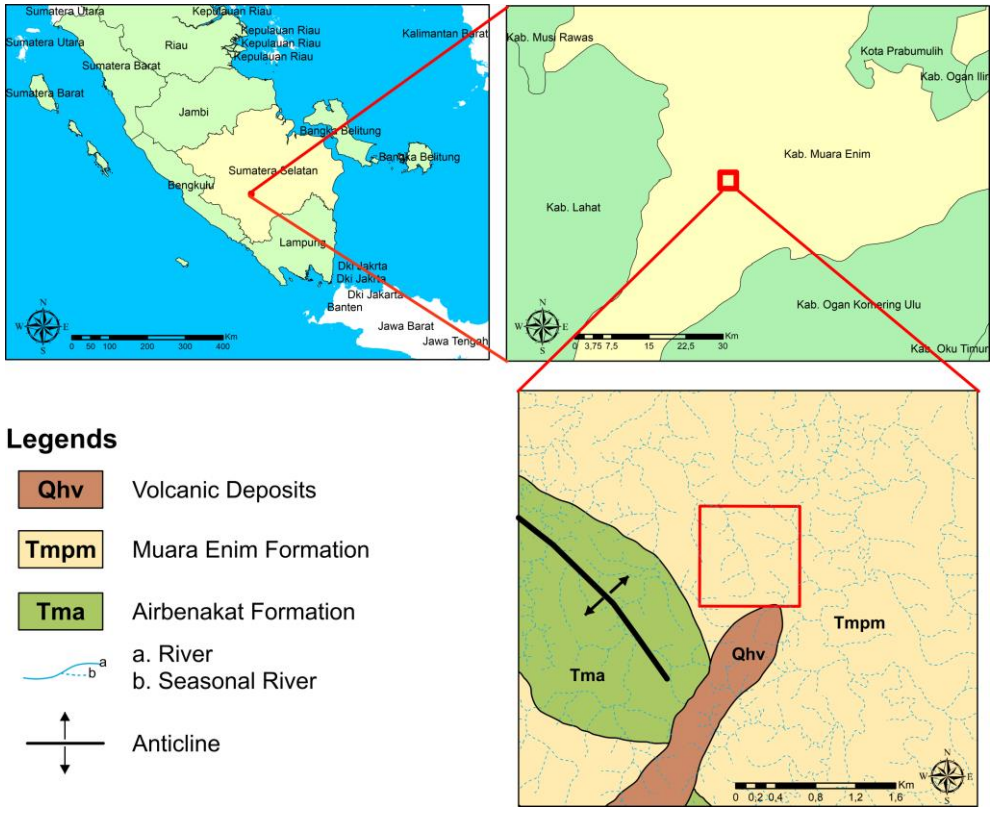

Figure 1. Research Location Map.

2. METHOD

The methods that we used in this study are geophysical log and core log analysis, single-factor and multi-factor analysis, and Inverse Distance Weight (IDW). The data used in this study was from four drill holes. In determining the type of lithofacies, sedimentary facies, and facies association, we use the lithological characteristics as proposed (Wang et al., 2011). System tracts and stratigraphic sequences were identified based on the presence of marine flooding surfaces (Wagoner et al. 1990a, 1990b). Sandstones are categorised as terrestrial to shallow marine sedimentary materials, while mudstones, shale, and claystone are categorised as deeper marine sedimentary materials. The system tracts composed of system tract boundaries at each drill hole were identified based on the explanation by Catuneanu (2017, 2020) and Ren et al. (2014).

When creating paleogeographic maps, we use single-factor and multi-factor comprehensive analysis methods (Lu et al., 2013). The single-factor analysis in this study involved contours of sandstone thickness, coal, and sand/shale ratio (Shao et al., 2020). Multi-factor analysis combines

single-factor analysis (Feng et al., 2014). The paleogeographic area was determined by the modified sand/shale ratio value from the previous study by Gao et al. (2022), Li et al. (2014); Shao et al. (2015, 2023); Zhu et al. (2022).

The Inverse Distance Weighting (IDW) method was used to analyse data from four drill holes and produce isopach maps for paleogeographic analysis, coal accumulation, and distribution. This method is commonly used to estimate values in unsampled areas by calculating a weighted average of surrounding sampled values (Herrero-Hernández et al., 2017).

3. RESULTS AND DISCUSSION

3.1. Sequence Stratigraphic Analysis of the M2 Member of the Muara Enim Formation

Sequence 1 in the research area starts with TST-1 and ends with HST-1 (**Figure 2**). The lithofacies deposited during TST-1 consisted of laminated shale, coal seam C, and lensed shale. The lithofacies of laminated and lensed shale appear to form a bell curve, indicating the formation of a fining-upward parasequence. In contrast, the coal lithofacies form a cylindrical curve, indicating an aggradation parasequence. The dominant fining-upward parasequence then forms a retrogradational parasequence set. The end of TST-1 is bounded by the maximum flooding surface-1 (MFS-1), which represents the highest point of sea level during sequence 1.

HST-1 was deposited after MFS-1 during the highstand phase. The deposition was marked by glauconite sandstone, lensed shale, and coal lithofacies. These lithofacies form a coarsening-upward parasequence which then forms a progradational parasequence set. The gamma-ray log shows that coal seam B2 formed a cylindrical pattern as a marker for the aggradational parasequence. The boundary between the end of sequence one and the beginning of the deposition of sequence two is marked by an erosional unconformity known as sequence boundary-1 (SB-1).

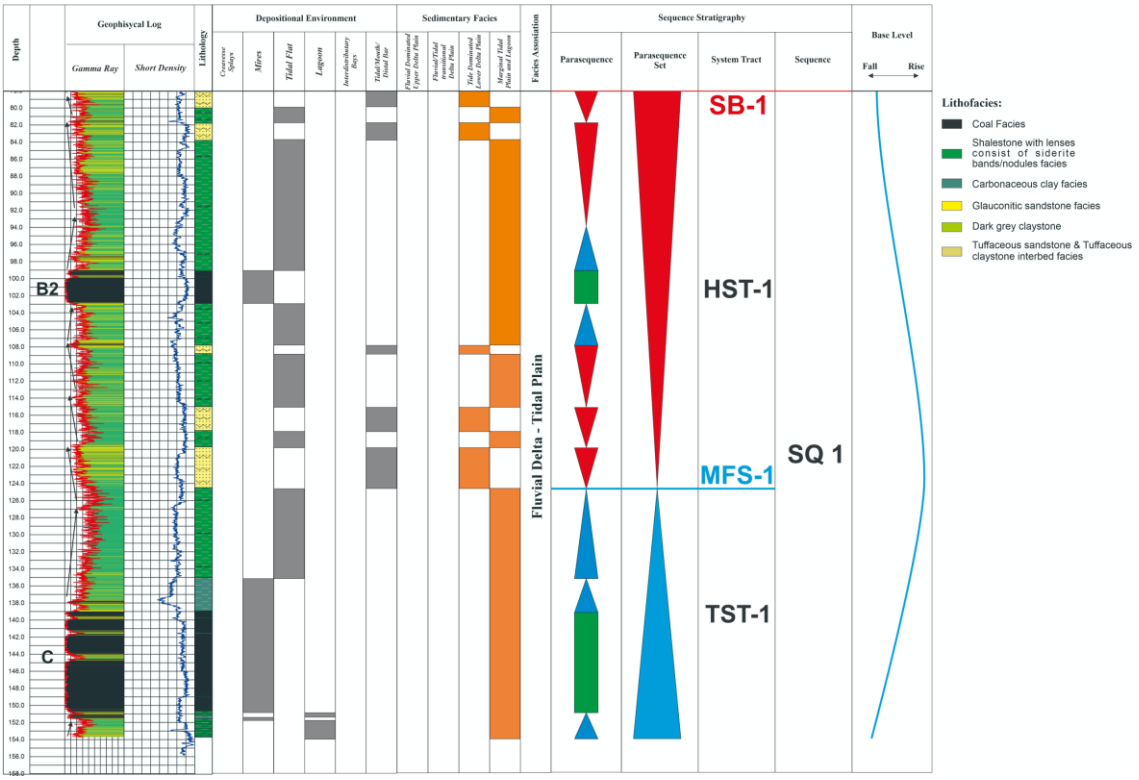

Figure 2. Sequence stratigraphy analysis of sequence 1 from KNH-03 drill hole.

Sequence 2 starts with TST-2 and ends with HST-2 (**Figure 3**). TST-2 comprises coal lithofacies (seam B1, Suban Marker, and A2) and laminated shale. The gamma-ray log shows that the coal lithofacies form cylindrical curves, indicating an aggradation parasequence. In contrast, the laminated shale lithofacies form a bell curve, indicating the formation of a fining-upward parasequence. TST-2 is dominated by fining-upward parasequences that form retrogradation

parasequences set during the transgression phase. The end of TST-2 is bounded by MFS-2 at its top, indicating the highest base level during sequence 2.

HST-2 is formed after the transgression phase and is bounded by MFS-1 at the bottom. It deposited coal seam A1 lithofacies, carbonaceous claystone, dark grey claystone, tuffaceous claystone and sandstone. The carbonaceous claystone lithofacies, as well as the tuffaceous claystone and sandstone, formed bell curves that create fining-upward parasequences. The coal seam A1 formed a cylindrical curve, and the dark grey mudstone formed a serrated curve, creating aggradational parasequences. The dominant aggradational parasequences formed an aggradational parasequence set that characterizes the HST-2. The end of HST-2 is bounded by SB-2, indicating the end of sequence 2 deposition.

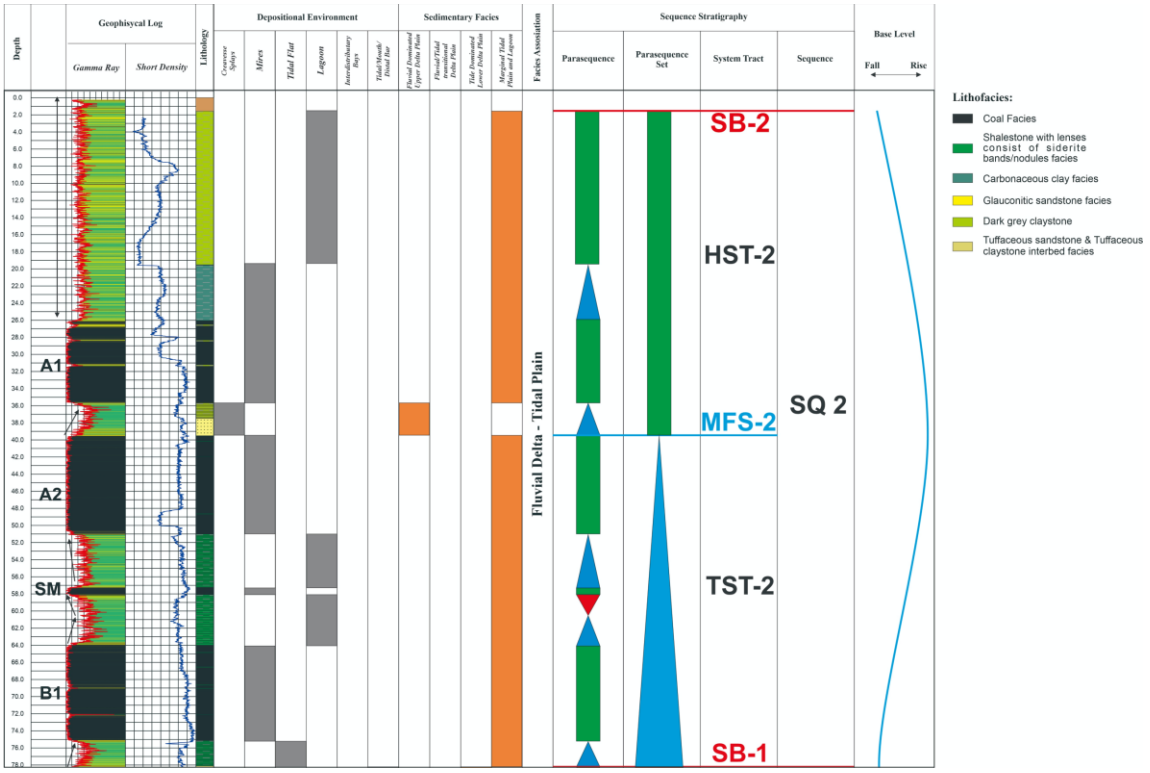

Figure 3. Sequence stratigraphy analysis of sequence 2 from KNH-03 drill hole**.**

3.2. Stratigraphic Sequence Evolution of the M2 Member of the Muara Enim Formation

3.2.1. Evolution of Sequence 1

Sequence 1 in the study area begins with TST-1 and ends with HST-1. The boundary between TST-1 and HST-1 is marked by Maximum Flooding Surface-1 (MFS-1), while the boundary between HST-1 and the overlying unit is marked by Sequence Boundary-1 (SB-1). During this period, most of the study area comprised lagoons, swamps, and mires. In the early TST-1, marine shale was deposited (see **Figure 4A**). It is inferred that the deposition occurred in a lagoon that belongs to the Tide Dominated Lower Delta Plain facies associated with the Fluvial Delta–Tidal Plain. The lithofacies were deposited as laminated dark grey shale with siderite bands. Laminae indicate weak depositional energy during lagoon conditions (Feng et al., 2021). The appearance of siderite was a result of iron-rich seawater conditions.

TST-1 represents the initial deposition mechanism at the research site for coal seam C. These coal facies formed in the middle of TST-1 (**Figure 4B**). The coal deposited in this system tract has continuous geometry (>1 Km), is very thick (11.35 to 12.00 m), tilted (> 20◦), and interspersed with 4 layers of clay bands impurities. The coal is thick and interspersed with thin clay bands, indicating disturbance by marine clay material carried by tidal currents over a short period.

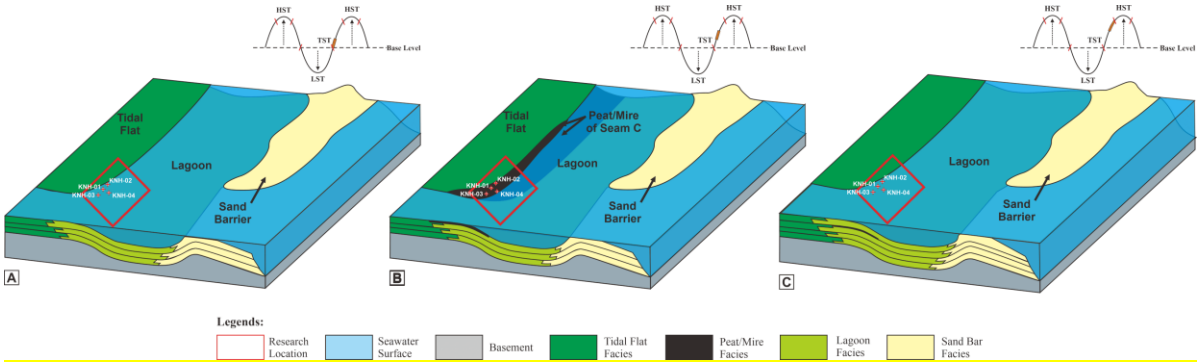

Figure 4. Deposition of sequence 1, TST-1: A) Early TST-1; B) Mid TST-1; C) End TST-1.

Coal accumulation ceased at the end of TST-1 due to the rising water level (**Figure 4C**). The increase in water level stopped coal accumulation and was followed by sedimentation of shallow marine clastic material in the form of carbonaceous mudstone and lagoon shale (Zhifei et al., 2020). The carbonaceous mudstone facies were deposited when the sea level rose before the underlying coal formation matured, mixing marine and organic materials.

At the beginning of HST-1, fine-grained glauconite sandstone lithofacies were deposited in a Tidal/Mouth/Distal Bars depositional environment. This environment is part of the Tide Dominated Lower Delta Plain facies and is associated with the Fluvial Delta-Tidal Plain facies (see **Figure 5A**). The sandstone lithofacies exhibit flaser, wavy, and lenticular bedding structures. The lithofacies formation mechanism during this time is interpreted to be influenced by the unidirectional tidal current transition from the Late TST-1 to the Early HST-1.

Marine sediment remains dominant in the middle of HST-1. The depositional environment is interpreted as a lagoon belonging to the Tide Dominated Lower Delta Plain facies associated with the Fluvial Delta – Tidal Plain. The deposited lithofacies comprise thin laminated shale with siderite bands or nodules, indicating a mixed system in the lagoon conditions (Tang et al., 2023). The high iron content in the seawater resulted in the presence of siderite minerals in these facies. The strong transgression-regression cycle of the current causes the formation of poorly sorted and imperfect nodular rocks (Tang et al., 2023). This condition leads to an increased supply of sediment in the form of organic material, exceeding the available accommodation space.

Consequently, the depositional environment changes from a lagoon to a swamp/mire (**Figure 5B**). Seam B2 was deposited during the HST-1. This coal seam has continuous geometric, moderately thick (3.72 to 4.30 m), gently inclined (18◦), and interspersed with a layer of clay band.

By the end of HST-1, the water level had continuously decreased, leading to an increased supply of sediment (sand materials) from the land to the sea. As the sea level decreases, sedimentation rates gradually increase compared to the rate of accommodation space formation (Liu et al., 2022). This triggers the development of clastic sediment deposition towards the basin, leading to a change in the swamp/mire environment to a tidal flat (see **Figure 5C**).

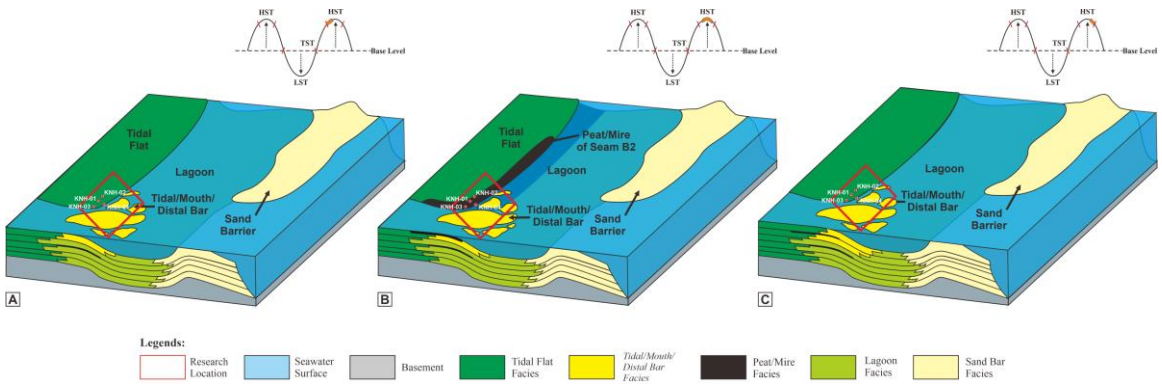

Figure 5. Deposition of sequence 1, HST-1: A) Early HST-1; B) Mid HST-1; C) End HST-1.

3.2.2. Evolution of Sequence 2

Sequence 2 is formed by a mechanism similar to that of sequence 1. It comprises two system tracts, which begin with TST-2 and HST-2 and are bounded by SB-1 at the bottom and SB-2 at the top. SB-1 marks the transition from the end of HST-1 to the beginning of TST-2 due to the deposition of shallow marine material in the form of lagoon shale.

In the early TST-2, deposition begins with the accumulation of lagoon shale. This material is characterised by a massive to laminated sedimentary structure, indicating decreased depositional energy at the research area. Deposition continues with the formation of thin coal. Suban marker is a thin coal (<1m) with a thickness ranging from 0.60 to 0.84m, continuous (>1 km), steeply inclined, with no interspersed, which is formed when the supply of peat-forming sediment is greater than the accommodation space for a short period (Abidin et al., 2022). The formation of the B1 coal seam, which is very thick (11.10 to 12.46 m), continuous (>1 Km), gently inclined (18◦), and contains 5 layers of clay bands, was caused by a decrease in deposition energy followed by an increase of accumulated organic materials (see **Figure 6A**). The formation of coal facies is related to the sensitivity of organic composition to the base level (Dai et al., 2020).

During the middle of TST-2, the seawater conditions were characterised by the direct cyclic deposition of iron-rich seawater due to the reduction in an organic-rich and acidic environment, resulting in the deposited shale containing siderite bands (Tang et al., 2023). This shale is part of the lagoon shale facies, included in the Marginal Tidal Plain and Lagoon facies, associated with the Fluvial Delta-Tidal Plain facies. The lack of sandstone deposits indicates that fine fraction material dominated deposition during this period (see **Figure 6B**).

As TST-2 ended and HST-2 began, sea level conditions increased significantly (see **Figure 6C**). Although a significant amount of accommodation space was formed, the peat accumulation rate balanced the accommodation space formation rate due to the abundance of coal-forming plants (Xu et al., 2020). This area became a swamp for the second time, accumulating coal seam A2 (Figure 6). The seam was thick (11.48 to 13.38 m), continuous (>1 km), steeply inclined (14◦), and interspersed with clay bands, indicating sea level interruption during coal deposition.

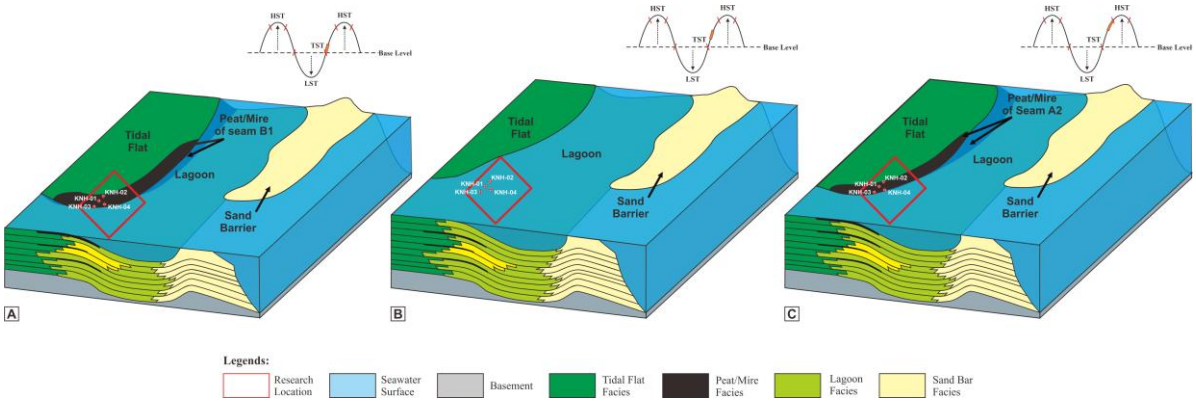

Figure 6. Deposition of sequence 2, TST-2: A) Early TST-2; B) Mid TST-2; C) End TST-2.

The transition from the end of TST-2 to the beginning of HST-2 started with the deposition of the tuffaceous sandstone facies. Due to a continuous and gradual rise in water levels. The crevasse splay (**Figure 7A**) formed due to tuffaceous sandstone initially deposited in floodplains in rivers or deltas being carried away by the overflowing water (Lepre, 2017). Over time, the crevasse splay expanded to cover the entire study area. This expansion also brought clay materials, which settled on top of the tuffaceous sandstone.

The tuffaceous sandstone is part of the Fluvial Dominated Upper Delta Plain, which is still associated with the Fluvial Delta – Tidal Plain facies. The Tuffaceous sandstone deposited in the crevasse splay during HST-2 has a thinner geometry. It is deposited widely, in contrast to the glauconite sandstone geometry produced by HST-1, which has a thicker, continuous geometry with a lensed structure due to its deposition in the tidal flat. The laminated/layered structure of the tuffaceous sandstone indicates that it was formed slowly with low depositional energy.

In the middle of HST-2, as the water level gradually decreased, organic sediment could balance the formation of accommodation space. Previously a crevasse splay, the research area became overgrown with plants and progressively became a swamp (see **Figure 7B**). The continuous accumulation of organic material in this region led to coal formation. Fluctuations in seawater cause the parent coal seam A to split, forming a continuous (>1 km), widespread, steeply inclined (16˚), and thick (9.40 to 9.60 meter) coal seam A1.

The deposition of massive mudstone and carbonaceous mudstone marked the end of HST-2. Carbonaceous mudstone is formed because immature coal-forming material is mixed with fine non-organic material carried by sea currents, formed after coal deposition with a thickness of 4.60-6.50 meters. The sea level, which continues to rise gradually, simultaneously carries and deposits clay material, causing the accumulation of organic material to stop, thus forming mudstone (**Figure 7C**). The depositional environment was transformed into a lagoon for the last time, and it is included in the Marginal Tidal Plain and Lagoon facies associated with the Fluvial Delta-Tidal Plain facies.

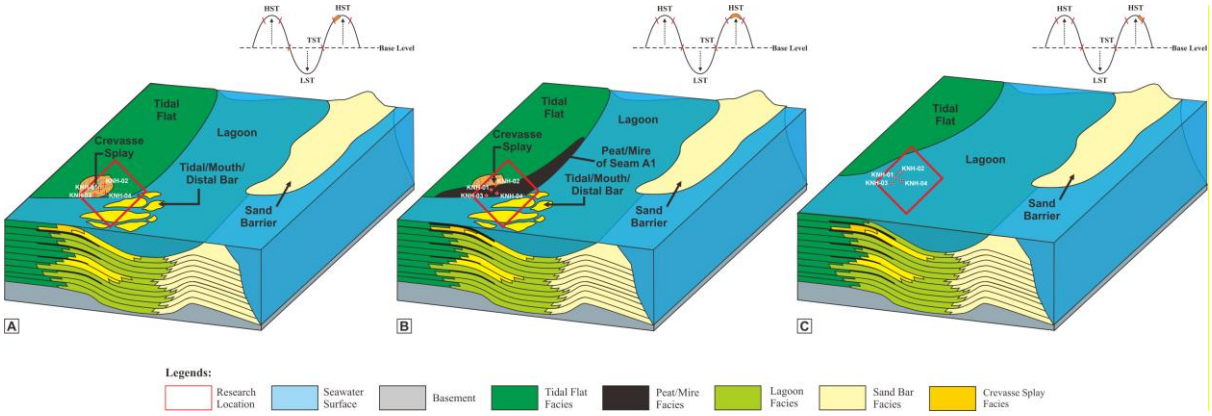

Figure 7. Deposition of sequence 2, HST-2: A) Early HST-2; B) Mid HST-2; C) End HST-2.

3.3. Paleogeographic Evolution M2 Member of the Muara Enim Formation

3.2.1. Palaeogeography of Sequence 1

Sequence 1 ranges in thickness from 74.82 to 84.30 meters. Its lithology comprises glauconite sandstone, dark gray shale with siderite nodules/bands, carbonaceous mudstone, and coal. The sandstone composition is dominated by glauconite minerals, which suggest shallow marine to terrestrial deposits (Torrado et al., 2020). Sequence 1 formed in a lagoon environment and later transformed into a tidal/mouth/distal bar and lagoon.

The isopach map of the sand/shale ratio aims to distinguish regions with high depositional energy that deposit coarse fraction rocks from those with low depositional energy that deposit fine fraction rocks (see **Figure 8A**). The deposition centres for the fine fraction are located at KNH-02 and KNH-04, with a ratio of 0.22 – 0.23, while the centres for the coarse fraction are at KNH-01 and KNH-03, with a ratio greater than 0.23. Isopach maps were created for each sequence to determine the extent and distribution of low-energy environments (Shao et al., 2020).

The lagoon and tidal/mouth/distal bar paleogeographic units formed in sequence 1 are balanced (**Figure 8B**). The overall thickness of shale deposited at the research location during this period ranges from 47.30 to 54.90 meters. The isopach map shows that the centre of shale accumulation is located in the Southeast (KNH-02) and Southwest (KNH-04), with a thickness ranging from 49.45 to 54.90 meters. The orientation of depositional currents in this period is South–North. Glauconite sandstone accumulates in the eastern part of the study area, specifically at KNH-01 and KNH-02, with a total thickness of 12.12 to 12.50 m. Sequence 1 contains two main seams, seam C and seam B2, with a total coal thickness of approximately 14 to 16.5 meters. The thickest coal is deposited at the tidal/mouth/distal bar. The thickness of coal seams is controlled by the balance between the capacity space and the rate of peat accumulation (Yan et al., 2021).

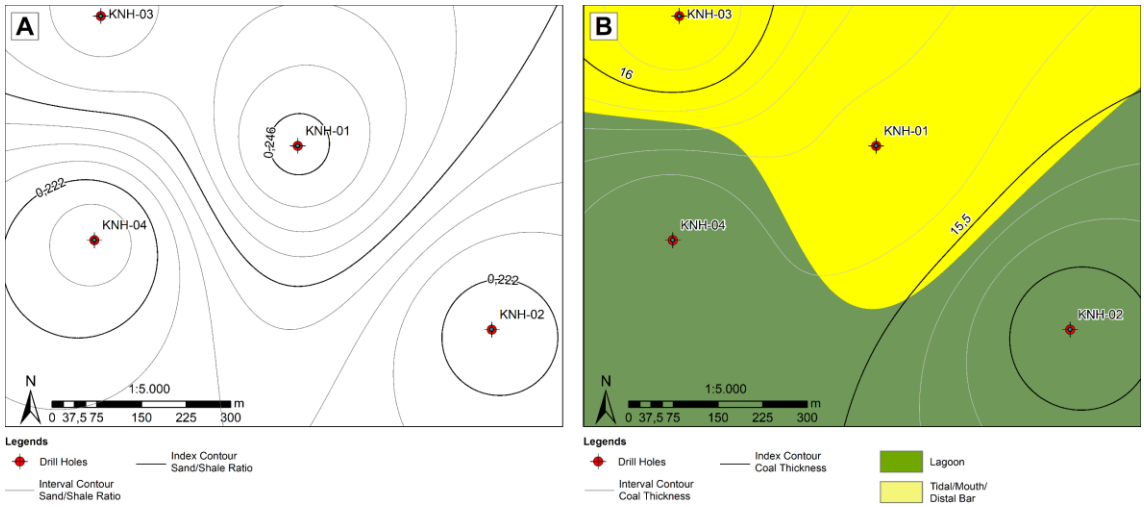

Figure 8. A) Sand/shale ratio map of sequence 1; B) Paleogeography map of sequence 1.

3.2.2. Palaeogeography of Sequence 2

Sequence 2 ranges in thickness from 73.56 to 90.20 meters. This sequence of lithology comprises tuffaceous sandstone, tuffaceous mudstone, dark grey shale with nodules/bands of siderite, carbonaceous mudstone, and coal. The sandstone is composed of quartz, biotite, and plagioclase, suggesting it combines volcanic materials. The tuffaceous mudstone above indicates that volcanic material in floodplain areas is carried by river currents during overflow (Lepre, 2017). This rock was deposited in the crevasse splay, as indicated by its sediment characteristics.

The sand/shale ratio isopach map illustrates the distribution of coarse and fine fraction material deposition during sequence 2 (**Figure 9A**). The fine-grained fraction centre is in KNH-03 and KNH-02, with a ratio of less than 0.047. Lagoon dominates the paleogeographic unit formed in sequence 2 (**Figure 9B**). During sequence 2, the mudstone thickness at the research location was approximately 38.30 to 52.30 meters. The isopach map shows that the centre of mudstone accumulation is in the southeast (KNH-02) and northwest (KNH-03), with a thickness ranging from 42.80 to 52.30 meters—the orientation of depositional current in southeast-northwest. In the research area, specifically at KNH-01 and KNH-04, tuffaceous sandstone has accumulated to a total thickness of 2.10 meters. Sequence 2 is the primary sequence for coal accumulation, as shown by the presence of three main seams: Suban Marker, seam B1, seam A2, and seam A1. The coal produced by sequence 2 has a total thickness range of around 33 to 39 meters, with the thickest coal deposited in the northwest and southeast areas. **Tables 1, 2, and 3** summarise the thickness of sandstone and mudstone, as well as the sand/shale ratio.

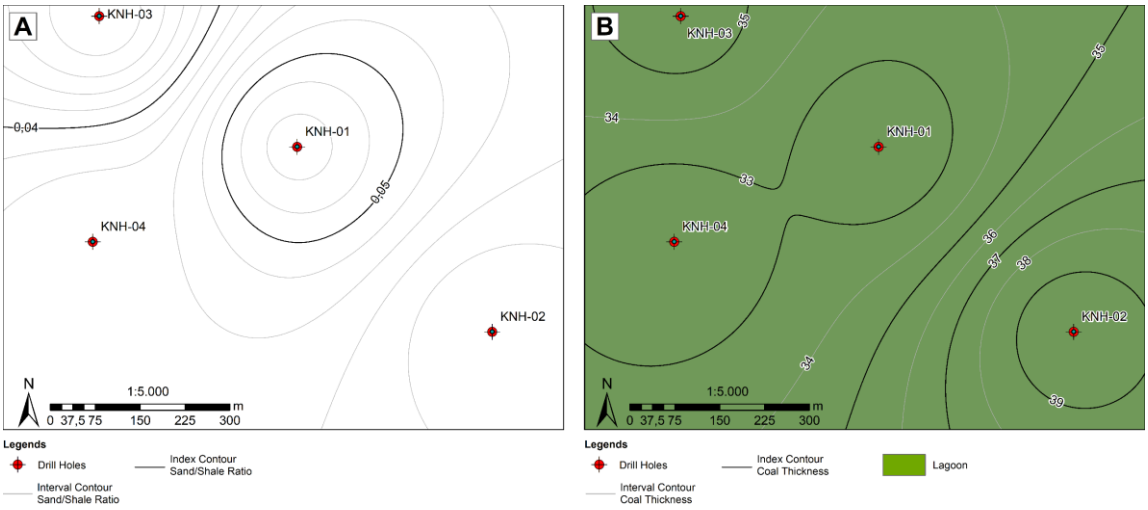

Figure 9. A) Sand/shale ratio map of sequence 2; B) Paleogeography map of sequence 2.

Table 1. Summary of sandstone thickness for each drill hole in HST-1 and HST-2.

Drill Holes	Thickness in Sequence 1 (m)	Thickness in Sequence 2 (m)
	HST-1	HST-2
KNH-01	12.50	2.10
KNH-02	12.12	1.73
KNH-03	11.40	1.60
KNH-04	10.75	2.10

Table 2. The total thickness of mudstone or shale for each drill hole in each system tract.

Drill Holes	Thickness in Sequence 1 (m)		Thickness in Sequence 2 (m)	
	TST-1	HST-1	TST-2	HST-2
KNH-01	17.48	33.10	12.10	26.20
KNH-02	23.60	31.30	15.80	27.00
KNH-03	20.50	26.80	18.30	34.00
KNH-04	22.35	27.10	17.55	28.50

Table 3. The sand/shale ratio and paleogeographic unit are in the research area.

Sequence	Drill Holes	Sand/Shale Ratio		Paleogeographic Unit
		Ratio	Percentage (%)	
1	KNH-01	0.2469	24.69	Tidal/Mouth/Distal Bar
	KNH-02	0.2208	22.08	Lagoon
	KNH-03	0.241	24.1	Tidal/Mouth/Distal Bar
	KNH-04	0.217	21.7	Lagoon
2	KNH-01	0.0548	5.48	Lagoon
	KNH-02	0.0404	4.04	Lagoon
	KNH-03	0.0306	3.06	Lagoon
	KNH-04	0.0456	4.56	Lagoon

The sedimentary environment of the M2 Member of Muara Enim Formation is classified into four categories based on research results, namely tidal-dominated lower delta plain, fluvial/tidal transitional delta plain, marginal tidal plain, and lagoon. This differs from the findings of other researchers, such as Amijaya and Littke (2005), who classified depositional environments into telmatic and limno-telmatic for ombrotrophic and mesotrophic conditions based on maceral composition. The results of this study also contrast with the findings of Elcofa et al. (2023), who classified depositional facies/environments into six categories, namely mixed flat, mouth bar, peat swamp, distributary channel, floodplain, and mudflat based on the lithological characteristic and its sedimentary structures. In general, it can be concluded that the study area is still part of the transitional lower delta plain environment, according to the analysis of Nasution and Nalendra (2017). The coal thickness in this research ranges from 0.60 to 0.84 m (thinnest) and about 13.38 m (thickest), which is slightly different from the coal thickness found by Algadri Nafian and Rizal (2021).

4. CONCLUSIONS

Four depositional environment settings are found: crevasse splay, mire/swamp, mudflat, lagoon, and tidal/mouth/distal bar. Three facies are sedimentary related to the fluvial delta-tidal plain: fluvial-dominated upper delta plain, tide-dominated lower delta plain, and marginal tidal plain and lagoon. Deposition in the study area consists of four system tracts, which are TST-1, HST-1, TST-2, and HST-2. Sequence 1 ranges in thickness from 74.82 to 84.30 meters and consists of glauconite sandstone, dark grey shale with siderite nodules/bands, carbonaceous mudstone, and coal. The paleogeographic units of the lagoon and tidal/mouth/distal bars formed in Sequence 1 are generally balanced. Tidal/mouth/distal bars develop in the northern part with a shale/sand ratio ranging from 0.217 to 0.247, while lagoon environments develop in the southern part. Sequence 2 ranges in thickness from 73.56 to 90.20 meters and consists of tuffaceous sandstone,

tuffaceous mudstone, dark grey mudstone, carbonaceous mudstone, and coal. The paleogeographic unit in sequence 2 consists of lagoons in the northwest and southeast, while the lagoon developed in the northeast-southwest direction with a sand/shale ratio ranging from 0.046 to 0.055. Sequence 2 is the most significant sequence for coal accumulation, as demonstrated by three primary seams: seam B1, seam A2, and seam A1.

5. ACKNOWLEDGMENTS

The authors would like to express our gratitude to Bukit Asam Tbk for providing facilities and legal permissions that contributed to this research. Also, thanks to all other people involved in this research, which cannot be mentioned in full.

6. REFERENCES

Abidin, N. S. Z., Mustapha, K. A., Abdullah, W. H., & Konjing, Z. (2022). Paleoenvironment Reconstruction and Peat-Forming Conditions of Neogene Paralic Coal Sequences from Mukah, Sarawak, Malaysia. *Scientific Reports*, *12*(1), 1–26. https://doi.org/10.1038/s41598-022-12668-6

Algadri Nafian, M., & Rizal, Y. (2021). Geologi Batubara Daerah Tanjung Enim, Kabupaten Muara Enim, Provinsi Sumatera Selatan. *Bulletin of Geology*, *5*(2), 589. https://doi.org/10.5614/bull.geol.2021.5.2.3

Amijaya, H., & Littke, R. (2005). Microfacies and Depositional Environment of Tertiary Tanjung Enim Low-Rank Coal, South Sumatra Basin, Indonesia. *International Journal of Coal Geology*, *61*(3–4), 197–221. https://doi.org/10.1016/j.coal.2004.07.004

Bai, Y., Lü, Q., Liu, Z., Sun, P., Liu, R., & Yao, S. (2020). Coal-Bearing Strata Sequence Stratigraphy of Paleogene Meihe Formation, Meihe Basin, NE China. *International Journal of Coal Science and Technology*, *8* (4), 547–561. https://doi.org/10.1007/s40789-020-00381-6

Buillit, N., Lallier-Vergè, E., Pradier, B., & Nicolas, G. (2002). Coal Petrographic Genetic Units in Deltaic-Plain Deposits of the Campanian Mesa Verde Group (New Mexico, USA). *International Journal of Coal Geology*, *51*, 93–110. www.elsevier.com/locate/ijcoalgeo

Catuneanu, O. (2017). Sequence Stratigraphy: Guidelines for a Standard Methodology. In M. Montenari (Ed.), *Stratigraphy & Timescales* (Vol. 2, pp. 1–57). Academic Press. https://doi.org/10.1016/bs.sats.2017.07.003

Catuneanu, O. (2020). Sequence Stratigraphy in The Context of The 'Modeling Revolution.' *Marine and Petroleum Geology*, *116*. https://doi.org/10.1016/j.marpetgeo.2020.104309

Dai, S., Bechtel, A., Eble, C. F., Flores, R. M., French, D., Graham, I. T., Hood, M. M., Hower, J. C., Korasidis, V. A., Moore, T. A., Püttmann, W., Wei, Q., Zhao, L., & O'Keefe, J. M. K. (2020). Recognition of Peat Depositional Environments in Coal: A review. *International Journal of Coal Geology*, *219*, 1–67. https://doi.org/10.1016/j.coal.2019.103383

Diessel, C., Boyd, R., Wadsworth, J., Leckie, D., & Chalmers, G. (2000). On Balanced and Unbalanced Accommodation/Peat Accumulation Ratios in the Cretaceous Coals from Gates Formation, Western Canada, and Their Sequence-Stratigraphic Significance. *International Journal of Coal Geology*, *43*, 143–186. www.elsevier.nlrlocaterijcoalgeo

Elcofa, D. G., Rochmana, Y. Z., Hastuti, E. W. D., & Gibran, M. A. K. (2023). Identifikasi Suksesi Delta Formasi Muaraenim Atas Daerah Tanjung Enim, Sumatera Selatan. *Journal of Geology Sriwijaya*, *2*(1), 1–5. http://ejournal.ft.unsri.ac.id/index.php/JGS

Feng, Y., Yang, Z., Zhu, J., Zhang, S., & Fu, X. (2021). Sequence Stratigraphy in Post-Rift River-Dominated Lacustrine Delta Deposits: A Case Study from the Upper Cretaceous Qingshankou Formation, Northern Songliao Basin, Northeastern China. *Geological Journal*, *56*(1), 316–336. https://doi.org/10.1002/gj.3948

Feng, Z. Z., Zheng, X. J., Bao, Z. D., Jin, Z. K., Wu, S. H., He, Y. Bin, Peng, Y. M., Yang, Y. Q., Zhang, J. Q., Zhang, Y. S., Wang, Y., & Liu, M. (2014). Quantitative Lithofacies

Palaeogeography. *Journal of Palaeogeography*, *3*(1), 1–34. https://doi.org/10.3724/SP.J.1261.2014.00001

Flint, S., Aitken, J., & Hampson, G. (1995). *Application of Sequence Stratigraphy to Coal-Bearing Coastal Plain Successions: Implications for the UK Coal Measures*. http://sp.lyellcollection.org/

Gao, Z., Shi, Y., Feng, J., Zhou, C., & Luo, Z. (2022). Lithofacies Paleogeography Restoration and Its Significance of Jurassic to Lower Cretaceous in Southern Margin of Junggar Basin, NW China. *Petroleum Exploration and Development*, *49*(1), 78–93. https://doi.org/10.1016/S1876-3804(22)60006-5

Hernández, A. H., Moro, F. J. L., Valle-Feijóo, M. E., Gómez-Fernández, F., & Rodríguez-Pérez, J. R. (2017). Mapping of Tecto-Lineaments and Their Influence on Sedimentological Processes in a GIS Environment: A Case Study of the Iberian Trough, Spain. *Geologica Carpathica*, *68*(2), 165–174. https://doi.org/10.1515/geoca-2017-0013

Lepre, C. J. (2017). Crevasse-Splay and Associated Depositional Environments of the Hominin-Bearing Lower Okote Member, Koobi Fora Formation (Plio-Pleistocene), Kenya. *The Depositional Record*, *3*(2), 161–186. https://doi.org/10.1002/dep2.31

Li, M., Shao, L., Lu, J., Spiro, B., Wen, H., & Li, Y. (2014). Sequence Stratigraphy and Paleogeography of the Middle Jurassic Coal Measures in the Yuqia Coalfield, Northern Qaidam Basin, Northwestern China. *AAPG Bulletin*, *98*(12), 2531–2550. https://doi.org/10.1306/06041413129

Liu, B., Chang, S., Zhang, S., Li, Y., Yang, Z., Liu, Z., & Chen, Q. (2022). Seismic-Geological Integrated Study on Sedimentary Evolution and Peat Accumulation Regularity of the Shanxi Formation in Xinjing Mining Area, Qinshui Basin. *Energies*, *15*(5). https://doi.org/10.3390/en15051851

Lu, J., Shao, L., Yang, M., Wang, H., & Qing, K. (2013). Sequence Paleogeography and Coal Accumulation in Epicontinental Basin. *International Journal of Mining Science and Technology*, *23*(6), 943–952. https://doi.org/10.1016/j.ijmst.2013.11.011

Luo, J. X., He, Y. Bin, Wang, R., Liu, M., & Hu, X. F. (2014). Lithofacies Palaeogeography of the Late Permian Wujiaping Age in the Middle and Upper Yangtze Region, China. *Journal of Palaeogeography*, *3*(4), 384–409. https://doi.org/10.3724/SP.J.1261.2014.00063

Nasution, F. P., & Nalendra, S. (2017). Characterization of Coal Quality Based On Ash Content From M2 Coal-Seam Group, Muara Enim Formation, South Sumatra Basin. *Journal of Geoscience, Engineering, Environment, and Technology*, *2*(3), 203. https://doi.org/10.24273/jgeet.2017.2.3.292

Opluštil, S., Šimůnek, Z., Zajíc, J., & Mencl, V. (2013). Climatic and Biotic Changes Around the Carboniferous/Permian Boundary Recorded in the Continental Basins of the Czech Republic. *International Journal of Coal Geology*, *119*, 114–151. https://doi.org/10.1016/j.coal.2013.07.014

Ren, J., Wang, H., Sun, M., Gan, H., Song, G., & Sun, Z. (2014). Sequence Stratigraphy and Sedimentary Facies of Lower Oligocene Yacheng Formation in Seepwater Area of Qiongdongnan Basin, Northern South China Sea: Implications for Coal-Bearing Source Rocks. *Journal of Earth Science*, *25*(5), 871–883. https://doi.org/10.1007/s12583-014-0479-6

Shao, L., Wang, X., Wang, D., Li, M., Wang, S., Li, Y., Shao, K., Zhang, C., Gao, C., Dong, D., Cheng, A., Lu, J., Ji, C., & Gao, D. (2020). Sequence Stratigraphy, Paleogeography, and Coal Accumulation Regularity of Major Coal-Accumulating Periods in China. *International Journal of Coal Science and Technology*, *7*(2), 240–262. https://doi.org/10.1007/s40789-020-00341-0

Shao, L. Y., Yang, Z. Y., Shang, X. X., Xiao, Z. H., Wang, S., Zhang, W. L., Zheng, M. Q., & Lu, J. (2015). Lithofacies palaeogeography of the Carboniferous and Permian in the Qinshui Basin, Shanxi Province, China. *Journal of Palaeogeography*, *4*(4), 384–412. https://doi.org/10.1016/j.jop.2015.06.001

Shao, Y., Zhao, F., Mu, G., Sun, B., Liang, K., Wang, D., Lu, J., Ma, S., & Shao, L. (2023). Sequence-Paleogeography and Coal Accumulation of the Late Carboniferous – Early Permian Paralic Successions in Western Shandong Province, Northern China. *Marine and Petroleum Geology*, *151*. https://doi.org/10.1016/j.marpetgeo.2023.106184

Shell Mijnbouw, N. V. (1976). *Geological Study of the Bukit Asam Coal Mines*.

Tang, H., Zhao, Q., Liu, B., Tan, S., & Shi, K. (2023). Types and Genesis of Siderite in the Coal-Bearing Beds of the Late Permian Xuanwei Formation in Eastern Yunnan, China. *Minerals*, *13*(9). https://doi.org/10.3390/min13091233

Torrado, L., Arenas, L. C. C., Mann, P., & Bhattacharya, J. (2020). Integrated Seismic and Well-Log Analysis for the Exploration of Stratigraphic Traps in the Carbonera Formation, Llanos Foreland Basin of Colombia. *Journal of South American Earth Sciences*, *104*, 1–27. https://doi.org/10.1016/j.jsames.2020.102607

Wagoner, J. C. Van, Mitchum, R. M., Campion, K. M., & Rahmanian, V. D. (1990a). Integrated Seismic and Well-Log Analysis for the Exploration of Stratigraphic Traps in the Carbonera Formation, Llanos Foreland Basin of Colombia. In *AAPG Methods in Exploration Series* (7th ed., Issue 7). The American Association of Petroleum Geologists.

Wagoner, J. C. Van, Mitchum, R. M., Campion, K. M., & Rahmanian, V. D. (1990b). Siliciclastic Sequence Stratigraphy in Well Logs, Cores, and Outcrops: Concepts for High-Resolution Correlation of Time and Facies. In *AAPG Methods in Exploration Series* (Vol. 7, Issue 7). The American Association of Petroleum Geologists.

Wang, H., Shao, L., Hao, L., Zhang, P., Glasspool, I. J., Wheeley, J. R., Wignall, P. B., Yi, T., Zhang, M., & Hilton, J. (2011). Sedimentology and Sequence Stratigraphy of The Lopingian (Late Permian) Coal Measures in Southwestern China. *International Journal of Coal Geology*, *85*(1), 168–183. https://doi.org/10.1016/j.coal.2010.11.003

Xu, X., Shao, L., Fu, Y., Wang, D., Cai, H., Qin, J., Hou, H., & Zhao, J. (2020). Sequence Palaeogeography, Lacustrine Basin Evolution, and Coal Accumulation in the Lower Cretaceous Fuxin Continental Faulted Basin, China. *Geological Journal*, *55*(2), 1195–1215. https://doi.org/10.1002/gj.3483

Yan, Z., Wang, J., & Wang, X. (2021). Sedimentary Environments and Coal Accumulation of the Middle Xishanyao Formation, Jurassic, in the Western Dananhu Coalfield, Turpan-Hami Basin. *Geofluids*, *2021*. https://doi.org/10.1155/2021/6034055

Zeng-Zhao Feng. (1999a). Origin, Development and Future of Palaeogeography of China. *Journal of Palaeogeography*, *1*(2), 1–7.

Zeng-Zhao Feng. (1999b). Struggle for Continuous Development and Innovation of Palaeogeography of China: Statement for Starting Publication of the Journal of Palaeogeography. *Journal of Palaeogeography*, *1*(1), 1–6.

Zhifei, L., Yingchun, W., Fanghui, H., Luoping, M., Xu, J., Rongfang, Q., & Daiyong, C. (2020). Control of Accommodation Changes Over Coal Composition: Case Study of Jurassic Medium-Thick Coal Seams in the Ordos Basin, China. *Arabian Journal of Geosciences*, *13*(5). https://doi.org/10.1007/s12517-020-5205-3

Zhu, M., Shao, L., Sun, B., Yao, H., Spina, A., Ma, S., Wang, S., Fan, J., Li, J. A., & Yan, S. (2022). Sequence Paleogeography and Coal Accumulation Model in the Fluvio-Lacustrine Rift Basin: The Lower Cretaceous of the Huhehu Sag of Hailar Basin, Inner Mongolia (NE China). *Marine and Petroleum Geology*, *145*. https://doi.org/10.1016/j.marpetgeo.2022.105879